DR. CAROLINA ALIAGA (Orcid ID : 0000-0002-1352-3164)

Article type : Special Issue Research Article

The Solvatofluorochromism of 2,4,6-Triarylpyrimidine Derivatives†

José Rodríguez-Aguilar,[1] Matías Vidal,[1] Camila Pastenes,[1] Carolina Aliaga,*[1,2]

Marcos Caroli Rezende[1] and Moisés Domínguez*[1]

[1] Facultad de Química y Biología, Universidad de Santiago de Chile, Av. Bernardo O´Higgins 3363, Santiago, Chile. [2] Centro para el Desarrollo de la Nanociencia y la Nanotecnología, CEDENNA, Chile

*Corresponding authors' e-mails: carolina.aliaga@usach.cl (Carolina Aliaga) and moises.dominguez@usach.cl (Moisés Dominguez)

†THIS ARTICLE IS PART OF A SPECIAL ISSUE DEDICATED TO DR. EDUARDO LISSI.

This article has been accepted for publication and undergone full peer review but has not been through the copyediting, typesetting, pagination and proofreading process, which may lead to differences between this version and the Version of Record. Please cite this article as doi: 10.1111/php.12982

ABSTRACT

Seven new 2,4,6-triarylpyrimidines were synthesized and their solvatofluorochromism investigated in 12 solvents and in an aqueous micellar solution of reduced Triton X-100. A multiparametric analysis of their emission band showed that the solvent dipolarity and basicity were mainly responsible for their solvatofluorochromism, which arose from an internal charge-transfer from a donor fragment to the pyrimidine acceptor, confirmed by theoretical calculations. In the micellar system, quenching of their fluorescence by addition of derivatives of 2,2,6,6-tetramethylpiperidinoxyl (TEMPO) radical was investigated, and the results were consistent with the spectral changes brought about by the micro-heterogeneous system.

INTRODUCTION

Electron-accepting pyridimines conjugated with different donor groups have been employed in the design of fluorescent probes. Such molecules, with a general formula A–π–D, exhibit interesting properties as solvent-sensitive emitting dyes. By varying the pyrimidine acceptor group A, the conjugating linkage π, or the donor group D, the solvatofluorochromic properties of these dyes can be widely varied. Examples of such variations include the direct linking between a pyrimidine ring and an amino group (1–3), conjugation of a pyridimidine system with a methoxyphenyl group (4), with an aminophenyl group linked through an ethylene bridge (5–8) or through an arylene (9), or heteroarylene spacer (10).

In a series of papers, Achelle *et al.* have synthesized and described the optical properties of a variety of fluorescent diazines of general formula A–π–D in homogeneous media (6–8, 11–13), arriving at general structure-activity relationships for these compounds (14).

In the present report we describe the synthesis and optical properties of a series of novel A–π–D solvatofluorochromic dyes **1a–g** (Scheme 1), investigating the effect of substituents X and Y on their spectral behavior.

A multiparametric analysis of their emission spectra in 12 solvents revealed the main properties responsible for the observed solvatofluorochromism. Their behavior was also investigated in an aqueous micellar solution of reduced Triton-X 100, by recording their spectra and by measuring the quenching of their fluorescence by addition of derivatives of 2,2,6,6-tetramethylpiperidinoxyl (TEMPO) radical.

MATERIALS AND METHODS

NMR spectra were recorded with a Bruker Avance 400 MHz equipment. IR spectra were measured with a Spectrum two FT-IR (ATR) Perkin Elmer spectrophotometer. Melting points were recorded with a Microthermal capillary melting-point apparatus and were not corrected.

All solvents employed for the spectral measurements were of spectroscopic grade. All reagents were analytically pure and were used without further purification. TLC analyses were performed on TLC plates (silica gel 60, fluorescence indicator F254, 0.25 mm layer thickness). Products were purified by column chromatography on silica gel 60 (0.063-0.200 mm). All reactions were carried out in standard oven-dried glassware.

The 4-acetoxy- and 4-hexanoyloxy-TEMPO derivatives were prepared following a reported procedure (15) Bromochalcones **4a**–**c** were synthesized according to literature procedures (16-18).

General procedure for the synthesis of pyrimidines 6a–c. A 20 mL round-bottom flask was charged with benzamidine hydrochloride **5** (440 mg, 2.8 mmol mmol) and the corresponding chalcone **4a**–**c** (2.8 mmol), potassium hydroxide (315 mg, 5.6 mmol) and ethanol (10 mL). The resulting mixture was heated at 120^{o} C for 1.5 h. Upon the end of the reaction (as observed on TLC, *n*-hexanes/EtOAc, 5:1), the solid that precipitated from the reaction mixture was separated by filtration, washed with cold ethanol and water and recrystallized from ethanol.

In this way, the following pyrimidines were prepared:

- ***4-(p-Bromophenyl)-2,6-diphenylpyrimidine (6a),*** obtained as a colorless solid (538 mg, 46%), mp 169–171 ºC (lit. (19) 168–170 ◦C). ^{1}H NMR (400 MHz, $CDCl_3$) δ: 7.62–7.53 (m, 7H), 7.69 (d, J = 8.34 Hz, 1H), 8.30–8.34 (m, 4H), 8.64–8.81 (m, 3H).
- ***4-(p-Bromophenyl)-6-(p-fluorophenyl)-2-phenylpyrimidine (6b),*** obtained as a colorless solid (715 mg, 63%), mp 127–129 ºC. ^{1}H NMR (400 MHz, $CDCl_3$) δ: 8.73–8.64 (m, 2H), 8.33–8.25 (m, 2H), 8.16 (d, J = 8.5 Hz, 2H), 7.92 (s, 1H), 7.69 (d, J = 8.5 Hz, 2H), 7.59–7.49 (m, 3H), 7.30–7.23 (m, 2H); ^{13}C NMR (101 MHz, $CDCl_3$) δ: not soluble enough to be recorded. FT–IR (ATR) v: 3070, 2925, 1590, 1550, 1375, 1195; HRMS (ESI–TOF): m/z $[M + H]^+$ calcd for $C_{22}H_{14}BrFN_2$: 405.0397; found: 405.0417.
- ***4-(p-Bromophenyl)-6-(p-methoxyphenyl)-2-phenylpyrimidine (6c),*** obtained as a light yellow solid (491 mg, 42%), mp 141-143 ºC. ^{1}H NMR (400 MHz, $CDCl_3$) δ: 8.73-8.65 (m, 2H), 8.28 (d, J = 8.8 Hz, 2H), 8.17 (d, J = 8.5 Hz, 2H), 7.92 (s, 1H), 7.69 (d, J = 8.5 Hz, 2H), 7.59–7.49 (m, 3H), 7.08 (d, J = 8.8 Hz, 2H), 3.92 (s, 3H); ^{13}C NMR (101 MHz, $CDCl_3$) δ: 164.5, 163.3, 162.1, 138.1, 136.6, 132.1, 131.5,

130.7, 130.3, 130.2, 129.8, 128.8, 128.8, 128.5, 128.4, 125.3, 114.3, 113.8, 109.1, 55.5; FT–IR (ATR) *v*: 3070, 2925, 1585, 1535; HRMS (ESI–TOF): *m*/*z* $[M + H]^+$ calcd for $C_{23}H_{17}BrN_2O$: 417.0597; found: 417.0612.

General procedure for the synthesis of dyes (1a–g). A microwave vial (10 mL) was charged with the bromophenyl-4-pyrimidines **6a**–**c** (0.7 mmol), $Pd(PPh_3)_4$ (41 mg ,0.035 mmol, 5 mol%), K_2CO_3 (97 mg, 0.7 mmol), *N*,*N*-dimethylformamide (5.0 mL), and 4-(*N*,*N*-dimethyl)phenylboronic acid (139 mg, 0.84 mmol) or the and 4-(*N*,*N*-diphenyl)phenylboronic acid (243 mg, 0.84 mmol). The resulting reaction mixture was heated for 1 h at 100 ºC. Upon the end of the reaction (as observed on TLC, *n*-hexanes/EtOAc, 5:1), the mixture was diluted with water (25 mL) and extracted with EtOAc (3 × 15 mL). The combined organic extracts were dried over Na_2SO_4 and all the volatile components were removed by rotary evaporation. The desired products **1a**–**g** were purified by column chromatography (*n*-hexanes:EtOAc, 20:1 → 5:1).

In this way, the following pyrimidines were prepared:

- ***2-Phenyl-4-[4-(4-N,N-dimethylaminophenyl)phenyl]-6-phenylpyrimidine (1a),*** obtained as a yellow solid (180 mg, 60%), mp 209–211 ºC. ^1H NMR (400 MHz, $CDCl_3$) *δ*: 8.77 – 8.73 (m, 2H), 8.34 (d, *J* = 8.4 Hz, 2H), 8.31 (dd, *J* = 7.8, 1.9 Hz, 2H), 8.05 (s, 1H), 7.76 (d, *J* = 8.4 Hz, 2H), 7.62 (d, *J* = 8.8 Hz, 2H), 7.58 – 7.52 (m, 6H), 6.84 (d, *J* = 8.8 Hz, 2H), 3.03 (s, 6H).; ^{13}C NMR (101 MHz, $CDCl_3$) *δ*: 164.6, 164.5, 150.4, 143.7, 137.7, 134.9, 133.2, 131.7, 130.7, 130.6, 129.3, 128.9, 128.7, 128.5, 128.4, 128.1, 127.8, 127.7, 127.3, 126.5, 112.7, 110.0, 44.7; FT–IR (ATR) *v*: 3070, 2960, 2870, 2805, 1620, 1590, 1510, 1230, 1090; HRMS (ESI-TOF): *m*/*z* $[M + H]^+$ calcd for $C_{30}H_{25}N_3$: 428.2121; found: 428.2133.

- ***2-Phenyl-4-[4-(4-N,N-dimethylaminophenyl)phenyl]-6-(4-fluorophenyl)pyrimidine (1b),*** obtained as a yellow solid (160 mg, 50%), mp 172–174 ºC. ^{1}H NMR (400 MHz, $CDCl_3$) δ: 8.77 – 8.68 (m, 2H), 8.36 – 8.27 (m, 4H), 7.99 (s, 1H), 7.75 (d, J = 8.5 Hz, 2H), 7.62 (d, J = 8.8 Hz, 2H), 7.58 – 7.50 (m, 4H), 7.29 – 7.21 (m, 1H), 6.88 – 6.82 (m, 2H), 3.03 (s, 6H); ^{13}C NMR (101 MHz, $CDCl_3$) δ: 164.7, 164.5, 163.5, 150.4, 143.7, 138.2, 134.8, 133.8, 130.9, 130.7, 129.4, 129.3, 128.8, 128.6, 128.5, 127.8, 127.7, 127.6, 126.5, 126.3, 116.0, 115.8, 112.7, 109.6, 40.5 (due to the very poor solubility of the product, the unambiguous determination of $J_{C\text{-}F}$ was not possible); FT–IR (ATR) v: 3055, 2965, 2870, 2800, 1615, 1595, 1520, 1230, 1085; HRMS (ESI-TOF): m/z $[M + H]^+$ calcd for $C_{30}H_{24}FN_3$: 446.2027; found: 446.2031.
- ***2-Phenyl-4-[4-(4-N,N-dimethylaminophenyl)phenyl]-6-(4-methoxyphenyl)pyrimidine (1c),*** obtained as a yellow solid (458 mg, 75%), mp 201–203 ºC. ^{1}H NMR (400 MHz, $CDCl_3$) δ: 8.78 – 8.69 (m, 2H), 8.32 (d, J = 8.4 Hz, 2H), 8.29 (d, J = 8.8 Hz, 2H), 7.97 (s, 1H), 7.74 (d, J = 8.4 Hz, 2H), 7.61 (d, J = 8.8 Hz, 2H), 7.57 – 7.49 (m, 3H), 7.07 (d, J = 8.8 Hz, 2H), 6.84 (d, J = 8.8 Hz, 3H), 3.91 (s, 3H); ^{13}C NMR (101 MHz, $CDCl_3$) δ: 164.4, 164.3, 164.1, 161.9, 150.4, 143.5, 138.5, 135.1, 130.5, 130.2, 128.8, 128.5, 128.4, 128.1, 127.8, 127.6, 126.4, 114.3, 112.7, 109.1, 55.6, 40.5; FT–IR (ATR) v: 3065, 2955, 2860, 2795, 1630, 1585, 1500, 1250, 1105; HRMS (ESI-TOF): m/z $[M + H]^+$ calcd for $C_{31}H_{27}N_3O$: 458.2227; found: 458.2237.
- ***2-Phenyl-4-[4-(4-N,N-diphenylaminophenyl)phenyl]-6-phenylpyrimidine (1d),*** obtained as a yellow solid (162 mg, 42%), mp 207–209 ºC. ^{1}H NMR (400 MHz, $CDCl_3$) δ: 8.79 – 8.70 (m, 2H), 8.36 (d, J = 8.1 Hz, 2H), 8.33 – 8.28 (m, 2H), 8.04 (s,

1H), 7.76 (d, *J* = 8.1 Hz, 2H), 7.60 – 7.50 (m, 8H), 7.30 (d, *J* = 7.8 Hz, 2H), 7.26 (d, *J* = 8.2 Hz, 2H), 7.20 – 7.13 (m, 6H), 7.09 – 7.02 (m, 2H).; ^{13}C NMR (101 MHz, $CDCl_3$) *δ*: 164.7, 164.5, 164.4, 147.6, 143.0, 138.2, 137.7, 135.8, 133.9, 130.8, 130.6, 129.4, 129.0, 128.5, 128.5, 127.8, 127.7, 127.3, 127.0, 124.7, 123.6, 123.2, 110.1.; FT–IR (ATR) ν: 3075, 2965, 2865, 2800, 1615, 1600, 1525, 1235, 1080; HRMS (ESI-TOF): *m*/*z* $[M + H]^+$ calcd for $C_{40}H_{29}N_3$: 552,2434; found: 552.2441.

- ***2-Phenyl-4-[4-(4-N,N-diphenylaminophenyl)phenyl]-6-(4-fluorophenyl)pyrimidine (1e),*** obtained as a yellow solid (279 mg, 70%), mp 163–165 ºC. ^{1}H NMR (400 MHz, $CDCl_3$) δ: 8.77 – 8.69 (m, 2H), 8.40 – 8.32 (m, 2H), 8.33 – 8.25 (m, 2H), 7.99 (s, 1H), 7.80 – 7.72 (m, 2H), 7.62 – 7.50 (m, 5H), 7.34 – 7.26 (m, 4H), 7.21 – 7.14 (m, 6H), 7.11 – 7.04 (m, 4H); ^{13}C NMR (101 MHz, $CDCl_3$) *δ*: 164.4, 164.2, 1623.0 (d, J^1 = 218 Hz), 147.8, 147.6, 142.9, 140.5, 138.4, 136.0, 133.9, 131.5, 130.5, 130.3 (d, J^3 = 5 Hz), 130.1, 129.4, 128.6 (d, J^2 = 35 Hz), 128.4, 127.8, 127.7, 127.0, 124.7, 123.6, 123.2, 114.3, 113.8, 109.2, 55.5; FT–IR (ATR) ν: 3065, 2975, 2870, 2795, 1620, 1595, 1520, 1220, 1075; HRMS (ESI-TOF): *m*/*z* $[M + H]^+$ calcd for $C_{40}H_{28}FN_3$: 570.2340; found: 570.2349.
- ***2-Phenyl-4-[4-(4-N,N-diphenylaminophenyl)phenyl]-6-(4-methoxyphenyl)pyrimidine (1f),*** obtained as a yellow solid (191 mg, 47%), mp 166–168 ºC.^{1}H NMR (400 MHz, $CDCl_3$) *δ*: 8.77 – 8.70 (m, 2H), 8.38 – 8.33 (m, 2H), 8.30 (d, *J* = 8.8 Hz, 2H), 7.99 (s, 1H), 7.76 (d, *J* = 8.4 Hz, 2H), 7.60 – 7.50 (m, 5H), 7.32 – 7.27 (m, 4H), 7.20 – 7.14 (m, 5H), 7.10 – 7.05 (m, 3H), 3.92 (s, 3H); Due to its very poor solubility, the ^{13}C NMR spectrum of the product was not recorded. FT–IR

(ATR) ν: 3080, 2970, 2865, 2790, 1615, 1595, 1510, 1210, 1095; HRMS (ESI-TOF): *m*/*z* $[M + H]^+$ calcd for $C_{41}H_{31}N_3O$: 582.2540; found: 582.2551.

- ***2-Phenyl-4-[4-(4-methoxyphenyl)phenyl]-6-phenylpyrimidine (1g),*** prepared by a coupling reaction with 4-methoxyphenylboronic acid (128 mg, 0.84 mmol). The product was obtained as a yellow solid (218 mg, 75%), mp 164-165 ºC. ^{1}H NMR (400 MHz, $CDCl_3$) δ: 8.74 (dd, *J* = 7.9, 1.9 Hz, 1H), 8.35 (d, *J* = 8.4 Hz, 1H), 8.33 – 8.26 (m, 1H), 8.04 (s, 0H), 7.74 (d, *J* = 8.5 Hz, 1H), 7.63 (d, *J* = 8.8 Hz, 1H), 7.60 – 7.49 (m, 3H), 7.02 (d, *J* = 8.7 Hz, 1H), 3.87 (s, 3H); ^{13}C NMR (101 MHz, $CDCl_3$) δ: 164.7, 164.5, 164.4, 159.7, 143.2, 138.3, 137.6, 135.8, 132.8, 130.8, 130.6, 128.9, 128.5, 128.5, 128.3, 127.7, 127.3, 127.1, 114.4, 110.1, 55.4; FT–IR (ATR) ν: 3080, 2975, 2870, 2795, 1620, 1590, 1510, 1215, 1075; HRMS (ESI-TOF): *m*/*z* $[M + H]^+$ calcd for $C_{29}H_{22}N_2O$: 415.1805; found: 415.1813.

Theoretical Calculations. All the quantum-chemical calculations were carried out with the Gaussian 09 package (20). Geometries for all molecules were optimized at the CAM-B3LYP/6-31+G(d) density-functional level of theory, and transition energies calculated with the TDDFT option. The Polarizable Continuum Model (PCM) was employed to mimic solvent effects for benzene, dichloromethane and dimethylsulfoxide.

Spectroscopic and photophysical measurements. UV–vis spectra were recorded on a Perkin Elmer Lambda 35 spectrophotometer in the range of 250–700 nm. Emission spectra were measured at room temperature (25 ±1^{o}C) on a Perkin Elmer LS 55 spectrofluorometer or a FluoroMax 4CP (Horiba Jovin Yvon). Fluorescence quantum yields were measured on a FluoroMax 4CP (Horiba Jovin Yvon) spectrofluorometer equipped with the Quanta-Phi integrating sphere.

RESULTS AND DISCUSSION

Synthesis of the diazines

Two synthetic approaches for building the pyrimidine ring in compounds like diazines **1a–g** have been described. The first of them employs condensation reactions from carbonyl (21-23) and carbonyl-masked compounds (24) of already functionalized starting materials. The second approach, a more flexible one, is based on the use of palladium-catalyzed cross-coupling reactions of chloropyrimidines (25-27) or pseudohalide derivatives (28).

The seven solvatofluorochromic diazines **1a**–**g** studied here were prepared by a combination of these two general approaches. The general synthetic route is shown in Scheme 2. Condensation of 4-substituted acetophenones **2a**–**c** with 4-bromobenzaldehyde provided the bromochalcones **4a**–**c** in very good yields (67-95%), which were cyclized to the 2,4,6-triphenylpyrimidine derivatives **6a-c** by reaction with benzamidine hydrochloride in moderate to good yields (42-63%). Finally, palladium-catalyzed Suzuki-Miyaura cross-coupling of **6a**–**c** with 4-*N*,*N*-diphenylamino-, 4-*N*,*N*-dimethylamino- or methoxyphenylboronic acid provided the solvatofluorochromic diazines **1a**–**g** in moderate to very good yields (42-75%).

Solvatofluorochromism of diazines 1a–g in pure solvents

The UV-Vis spectra of diazines **1a–g** showed weak absorptions in the range of 400-330 nm, with maxima that were not resolved in most solvents, similarly to reported spectra of triarylpyrimidines (29, 30). These broad ICT bands were composite, as shown by the two excitation bands at 331 and 371 nm, obtained from the emission spectrum of **1a** in DMSO

(Figure 1). By contrast with the corresponding emission bands, the lower-energy absorption band was not strongly solvent-dependent, with maxima at 358 nm in hexane, 363 nm in methanol and 371 nm in DMSO. Following the suggestion of Kido *et al.* in their detailed study of the emission spectra of some triarylpyrimidines (29), we assigned the more intense, fluorosolvatochromic emission band with the lower-energy absorption to a normal ICT process. The higher-energy band at 331 nm in DMSO possibly originated from a TICT process (1-3). A detailed confirmation of this hypothesis in all employed solvents was however beyond the scope of the present work.

In their emission spectra, the intense, solvent-dependent band shifted, in the case of dyes **1a**–**c**, from 425-430 nm in hexane to 550-565 nm in DMSO. In the case of the *N*,*N*-diphenylamino derivatives **1d**–**f** , this emission band shifted from 430-435 nm in hexane to 535-540 nm in methanol. Finally, for dye **1g**, a shorter solvatofluorochromic range was observed, from 379 nm in hexane to 461 nm in methanol. A representative example of their behavior is reproduced for diazine **1a** in Figure 2.

Emission energy values in kcal.mol^{-1} ($E_{em} = 28590 / \lambda_{max}^{em}$) for all diazines **1a**–**g** in twelve solvents of a wide range of polarities are listed in Table 1. Water was excluded from the set of studied solvents, because of the erratic behavior of the emission band of all diazines in this rather acidic solvent, a probable reflection of the strong hydrogen-bonds between the solutes and this medium.

In the search of the solvent properties responsible for the observed solvatofluorochromism of the studied diazines, a multiparametric regression analysis of their emission energies was performed employing Equation 1 and Catalán's parameters for solvent acidity (SA), basicity (SB), polarizability (SP) and dipolarity (SdP) (31).

$$E_{em}^{calc} = E_{em}^{0} + a\,SA + b\,SB + c\,SP + d\,SdP \qquad (1)$$

The resulting values from the regression analysis for the corresponding coefficients *a*, *b*, *c* and *d* are given in Table 2.

According to the results of the multiparametric regression in Table 2, the solvatofluorochromism of diazines **1a–g** depends mainly on the solvent dipolarity SdP, being also affected by the medium polarizability (SP) and basicity (SB). The medium acidity has only a minor influence on the solvatofluorochromic behavior.

Diazines **1a–g** can be described as resonance hybrids of the two canonical formulae (**I**) and (**II**), where (**I**) is the major contributor to the ground state and (**II**) to the excited state (Scheme 3). The canonical structure (**II**) is stabilized by dipolar, basic solvents, resulting in a reduction of the emission energy from this new less energetic state.

Solvent dipolarity is the major contributor for the stabilization of canonical structure (**II**), with the larger negative coefficient *d* that varies little in the analogous series **1a**–**f**. Replacement of the amino group by the less electron-donating methoxy group in **1g** reduces the contribution of (**II**) to the excited-state resonance hybrid. Accordingly, the absolute value of coefficient *d* is also reduced.

The influence of the medium basicity and polarizability on the internal charge-transfer of the amino derivatives **1a–1f** depends on the nature of the electron-donor and of substituent R. Both the NMe_2 and the NPh_2 donor groups stabilize the canonical structure (**II**) by electrostatic attraction between the solvent and the positive end Y of the solute, which

is reflected in a high sensitivity to the medium basicity. Steric hindrance by the bulky phenyl rings, which shields the positive end Y in structure (**II**) from the solvent, can nevertheless reduce the sensitivity of compounds **1d**–**f** to the medium basicity. In addition, as a more polarizable group than NMe_2, the NPh_2 donor leads to dyes with larger sensitivities to the medium polarizability (coefficient *c* of equation 1) than dyes **1a**–**c**, with a *N*,*N*-dimethylamino donor.

The results obtained with the aid of Eq. 1 were validated by the good correlation obtained between the experimental (E_{em}^{exp}) and the calculated emission energy values (E_{em}^{calc}), obtained from the simplified equation 2, which considered only the two parameters largely responsible for the observed solvatofluorochromism of these dyes, solvent basicity SB and dipolarity SdP.

$$E_{em}^{calc} = E_{em}^{0} + b\,SB + d\,SdP \qquad (2)$$

Values for the fitting parameters E_{em}^{0}, *b* and *d* of equation 2 are given in Table 2. As an example, Figure 3 illustrates the good correlation ($r^2 = 0.97$) obtained by plotting the calculated emission energies from equation 2 against the experimental values for diazine **1a**.

The fitting parameter E_{em}^{0} should correspond to emission energies from spectra of dyes **1a-g** in the gas phase. These values should be very similar to the E_{em} values in the least polar solvent of the set (hexane). In fact, comparison of the E_{em}^{0} values of equation 2 (Table 2) with the corresponding emission energy values in hexane (Table 1) reveals very small differences, with deviations that are not greater than ± 0.9 $kcal.mol^{-1}$.

The rather small variation of the regression parameters *a*, *b* and *c* in the series of diazines **1a**–**g** is in agreement with the two structural features previously stressed by Achelle *et al.* in a comprehensive study of structure-property relationships of different emitting diazines (14). Both the nature of the Y group, which should affect the 1,3-diazine moiety, or the nature of the X group, which should affect the 4-aminophenyl fragment, play a relatively unimportant role in the solvatofluorochromism of these compounds.

Computational calculations in pure solvents

TDDFT calculations of the emission spectra of diazine **1a** were carried out to shed light on the nature of its solvatofluorochromic band. As suggested by Jacquemin *et al.* for similar diazines (32) we have employed the range-separated hybrid CAM-B3LYP for the geometry optimizations of the ground (S_o) and excited state (S_1). The structures of both states showed a high coplanarity between the pyrimidine, the phenyl-linkage and the *N*,*N*-dimethylaminophenyl rings.

The calculated emission energies of diazine **1a** shown in Table 1 were obtained as the energetic difference between the ground and the first excited state, after relaxation of the excited structure. After optimization of the ground state structure at the CAM-B3LYP/6-31+G(d) level of theory, the first excited state was obtained and relaxed with the aid of the TDDFT method at the same level of theory. The Polarizable Continuum Model (PCM) was employed to mimic the solvent effect for benzene, dichloromethane and dimethyl sulfoxide (20).

The calculated emission energies in benzene, dichloromethane and dimethylsulfoxide are given in Table 3.

The calculated emission energies of diazine **1a** in the three solvents are very close to those observed experimentally, differing only by 2-6 kcal.mol^{-1}. This good agreement supports the idea of a planar excited state and of an ICT $S_1 \rightarrow S_o$ transition as responsible for the solvatofluorochromic band.

The nature of the emission band was studied by analysing the electron densities of the ground and the excited state of diazine **1a**. Figure 4 shows that charge is transferred from the donor *N*,*N*-dimethylaminophenyl group to the pyrimidine acceptor ring. Internal charge-transfer occurs along the main axis of the molecule, involving the substituent at the 4-position of the pyrimidine system, with little participation of the 2- and 6- phenyl substituents. A very similar charge flow could be observed in benzene and dimethylsulfoxide.

Fluorescence and quenching in a micellar system

The observed solvatofluorochromism of the pyrimidine dyes **1a**–**g** suggested a comparison of this behavior in pure solvents and in a micellar system. The poor solubility of these dyes in water was an indication of their hydrophobicity, and of a more effective solubility in micellar media. In fact, in an aqueous solution of a neutral micelle (reduced Triton X-100), the solubility of dyes **1a** and **1d** increased significantly, allowing reliable emission spectra of these two compounds to be recorded in aqueous media and compared with their fluorescence spectra in pure solvents.

Table 4 lists the emission λ_{max} values for the two dyes in an aqueous solution of Triton X-100, together with the corresponding quantum yields in this medium. For the sake of comparison, quantum yields for the two dyes were also determined in methanol and in benzene, and are included in the table.

Values for the fluorescence maxima of dyes **1a** and **1d** in the neutral micellar system (452 nm) are similar to the corresponding λ_{max} values obtained in benzene (454 nm for **1a** and 444 nm for **1d**), suggesting that the two dyes are located in the more hydrophobic core of the micelle, in a microenvironment with a polarity similar to that of non-polar benzene. A similar conclusion is reached by comparison of the quantum yields of the two dyes in the micellar system with those in benzene. Quantum yields in this pure non-polar solvent were similar and only slightly larger (0.758 or **1a** and 1.000 for **1d**) than in the micro-heterogeneous system (0.559 for **1a** and 0.878 for **1d**).

An alternative approach for determining the location of the two dyes in the micellar micro-environment was the application of a recently developed protocol for locating antioxidants in these media. The protocol was based on the comparative quenching ability of an antioxidant in a micellar medium *vis-à-vis* a series of radical TEMPO derivatives of increasing hydrophobicity (33).

In the present work the protocol was simplified to the use of only two analogous TEMPO derivatives of different hydrophobicities, compounds **12a** and **12b**

Addition of increasing amounts of any of the two radicals quenched the fluorescence of dyes **1a** and **1d** in the micelle. Linear Stern-Volmer plots were obtained in all cases (Figure 5) allowing the determination of quenching constants for the two dyes towards radicals **12a** or **12b**.

Table 5 lists the Stern-Volmer constants obtained for the two dyes in the micelle, in the presence of radicals **12a** and **12b**.

For both dyes **1a** and **1d**, the more hydrophobic radical **12b** was a more effective quencher, suggesting a closer proximity between the dyes and this hydrophobic quencher in the micelle. This was in agreement with the evidence from the data of Table 4, which suggested that the two dyes were located in a hydrophobic environment within the micelle. In addition, **1d** showed a greater sensitivity to the hydrophobic nature of the quenchers than **1a.** This is shown in a comparison of the Stern-Volmer constants of **1a** and **1d** in Table 5. Changing from **12a** to the more hydrophobic quencher **12b** resulted in a 1.3-fold increase of the Stern-Volmer constant for dye **1a** and of a 1.6-fold increase for dye **1d**. This observation suggested that dye **1d**, being more hydrophobic than **1a,** was located in a more hydrophobic micro-environment within the micelle than dye **1a.** This conclusion too was in agreement with the data of Table 4, which suggested a more hydrophobic micro-environment for dye **1d** (a larger quantum-yield value) than for dye **1a**.

CONCLUSIONS

A series of 2,4,6-triarylpyrimidines were synthesized and their solvatofluorochromic behavior investigated in pure solvents and in an aqueous micellar solution of reduced Triton X-100. The existence of composite emission bands for all dyes was suggested by the emission spectrum of **1a** in DMSO and in micelle solutions. The major band in these media was ascribed to an internal charge-transfer process, as revealed by theoretical calculations. This solvatofluorochromic band exhibited variations of its Stokes shift as large as 124 nm, as shown, for example, by the spectra of compound **1a** in hexane (shift of 67 nm) and in DMSO (shift of 191 nm). Quantum yields as large as 1.00 were

observed in non-polar benzene, decreasing significantly in protic solvents. In a micellar solution of reduced Triton X-100, quantum yields were as large as in non-polar media.

A multiparametric regression analysis of their spectral behavior in 12 solvents, employing Catalán's parameters (31). revealed a major dependence of their emission band on the solvent dipolarity and basicity, with some contribution in the case of the *N*,*N*-diphenylamino derivatives **1d–f** of the solvent polarizability. These trends were rationalized by the existence of a dipolar excited state, stabilized by polarizable, basic solvents.

The poorly soluble dyes in water were readily solubilized in an aqueous micellar solution of reduced Triton X-100. Two analogous dyes, **1a** and **1d**, with a *N*,*N*-dimethylamino- or a *N*,*N*-diphenylamino substituent, had their fluorescence spectra recorded in this micellar system. Their fluorescence quenching by two derivatives of the TEMPO radical was also studied in this neutral micellar medium. The emission λ_{max} values and the quantum yield for the two dyes in this medium were consistent with the corresponding Stern-Volmer quenching constants determined in the micelle. These data pointed to slightly different locations of the two dyes within the micelle, with the more hydrophobic *N*,*N*-diphenylamino derivative **1d** lodging in a more hydrophobic microenvironment in the micelle than its *N*,*N*-dimethylamino analog **1a**.

ACKNOWLEDGEMENTS*:* Financial support from FONDECYT projects 11140497 and 1140212 is gratefully acknowledged. M. V. thanks USA1555 project from VRIDEI-USACH. CA thanks CEDENNA PB0807 project. We thank Dr. N. Pizarro (UNAB) for helping us with quantum-yield measurements.

REFERENCES

1. Herbich, J., Z. R. Grabowski, H. Wojtowicz, K. Golankiewicz (1989) Dual fluorescence of 4-(dialkylamino)pyrimidines. Twisted intramolecular charge transfer state formation favored by hydrogen bond or by coordination to the metal ion. J. Phys. Chem. 93, 3439–3444. DOI: 10.1021/j100346a015.
2. Herbich, J., F. P. Salgado, R. P. H. Rettschnick, Z. R. Grabowski and H. Wójtowicz (1991) "Twisted" Intramolecular Charge-Transfer States in Supercooled Molecules: Structural Effects and Clustering with Polar Molecules. J. Phys. Chem. 95, 3491-3497. DOI: 10.1021/j100162a011
3. Herbich, J. and J. Waluk (1994) Excited charge transfer states in 4-aminopyrimidines, 4-(dimethylanilino)pyrimidine and 4-(dimethylamino)pyridine. Chem. Phys. 188, 247-265. DOI: 10.1016/0301-0104(94)00256-8.
4. Suryawanshi, V. D., A. H. Gore, L. S. Walekar, P. V. Anbhule, S. R. Patil and G.B. Kolekar (2013) Solvatochromic fluorescence behavior of 2-amino-6-hydroxy-4-(3,4-dimethoxyphenyl)-pyrimidine-5-carbonitrile: A sensitive fluorescent probe for detection of pH and water composition in binary aqueous solutions, J. Mol. Liq. 184, 4-9. DOI: 10.1016/j.molliq.2013.03.018.
5. Liu, B., H-L. Zhang, J. Liu, Y.-D. Zhao, Q.-M. Luo and Z.-L. Huang (2007) Novel pyrimidine-based amphiphilic molecules: synthesis, spectroscopic properties and applications in two-photon fluorescence microscopic imaging. J. Mater. Chem.17, 2921-2929. DOI: 10.1039/B702004J.
6. Hadad, C., S. Achelle, J. C. García-Martinez and J. Rodríguez-López (2011) 4-Arylvinyl-2,6-di(pyridin-2-yl)pyrimidines: Synthesis and Optical Properties. J. Org. Chem. 76, 3837-3845. DOI: 10.1021/jo200204u.

7. Achelle, S., A. Barsella, C. Baudequin, B. Caro and F. Robin-le Guen (2012) Synthesis and Photophysical Investigation of a Series of Push–Pull Arylvinyldiazine Chromophores. J. Org. Chem. 77, 4087-4096. DOI: 10.1021/jo3004919.
8. Achelle, S., F. Robin-le Guen (2013) 2-Arylvinylpyrimidines versus 4-arylvinylpyrimidines: synthesis and comparison of the optical properties, Tetrahedron Lett. 54, 4491-4496. DOI: 10.1016/j.tetlet.2013.06.040
9. Weng, J., Q. Mei, Q. Fan, Q. Ling, B. Tong, W. Huang (2013) Bipolar luminescent materials containing pyrimidine terminals: synthesis, photophysical properties and a theoretical study. RSC Adv. 3, 21183-21191. DOI: 10.1039/c3ra43631d.
10. Verbitskiy, E. V., A. A. Baranova, K. I. Lugovik, M. Z. Shafikov, K. O. Khokhlov, E. M. Cheprakova, G. L. Rusinov, O. N. Chupakhin, V. N. Charushin (2016) Detection of nitroaromatic explosives by new D-π-A sensing fluorophores on the basis of the pyrimidine scaffold. Anal. Bioanal. Chem. 408, 4093-4101. DOI: 10.1007/s00216-016-9501-4
11. Achelle, S., I. Nouira, B. Pfaffinger, Y. Ramondenc, N. Plé and J. Rodriguez-López (2009) V-Shaped 4,6-Bis(arylvinyl)pyrimidine Oligomers: Synthesis and Optical Properties, J. Org. Chem. 74, 3711-3717. DOI: 10.1021/jo900107u.
12. Achelle, S., J. Rodríguez-López and F. Robin-le Guen (2018) Photolumiscence Properties of Aryl-, Arylvinyl-, and Arylethynylpyrimidine Derivatives, ChemistrySelect, 3, 1852-1886. DOI: 10.1002/slct.201702472.
13. Klikar, M., P. le Poul, A. Růžička, O. Pytela, A. Barsella, K. D. Dorkenoo, F. Robin-le Guen, F. Bureš and S. Achelle (2017) Dipolar NLO Chromophores Bearing Diazine Rings as π–Conjugated Linkers. J. Org. Chem. 82, 9435-9451. DOI: 10.1021/acs.joc.7b01442.

14. Achelle, S., F. Robin-le Guen (2017) Emission properties of diazines chromophores: Structure-properties relationship. J. Photochem. Photobiol. A 348 281-286. DOI: 10.1016/j.jphotochem.2017.08.060.
15. Aliaga, C. F. Bravo-Moraga, D. Gonzalez-Nilo, S. Márquez, S. Lühr, G. Mena and M. C. Rezende. (2016) Location of TEMPO derivatives in micelles: subtle effect of the probe orientation. Food Chem. 192, 395-401. DOI: org/10.1016/j.foodchem.2015.07.036.
16. Raghav, N., M. Singh (2014) SAR studies of differently functionalized chalcones based hydrazones and their cyclized derivatives as inhibitors of mammalian cathepsin B and cathepsin H. Bioorg. Med. Chem. 22, 4233-4245. DOI: 10.1016/j.bmc.2014.05.037.
17. Thirunarayanan, G. and G. Vanangamudi (2014) Synthesis, spectral studies, antimicrobial and insect antifeedant activities of some substituted styryl 4′-fluorophenyl ketones. Arab. J. Chem. 7, 1055-1064. DOI: 10.1016/j.arabjc.2010.10.034.
18. Gezegen, H. and M. Ceylan (2015) Synthesis of 3,5-Diarylcyclohex-2-enones by NH_4Cl/Hcl-Catalyzed Cyclization and Deacetylation of 4-Acetylhexane-1,5-diones. Helv. Chim. Acta 98, 253-259. DOI: 10.1002/hlca.201400168.
19. Kong, K.-H., Y. Chen, X. Ma, K. C. Wai and Y. Lam, (2004) Traceless Solid-Phase Synthesis of Nitrogen-Containing Heterocycles and Their Biological Evaluations as Inhibitors of Neuronal Sodium Channels J. Comb. Chem. 2004, 6, 928–933. DOI: 10.1021/cc049910t.
20. Gaussian 09, Revision A.02, M. J. Frisch, G. W. Trucks, H. B. Schlegel, G. E. Scuseria, M. A. Robb, J. R. Cheeseman, G. Scalmani, V. Barone, G. A. Petersson, H. Nakatsuji, X. Li, M. Caricato, A. Marenich, J. Bloino, B. G. Janesko, R. Gomperts, B. Mennucci, H. P. Hratchian, J. V. Ortiz, A. F. Izmaylov, J. L. Sonnenberg, D. Williams-Young, F. Ding, F. Lipparini, F. Egidi, J. Goings, B. Peng, A. Petrone, T. Henderson, D. Ranasinghe, V. G. Zakrzewski, J. Gao, N. Rega, G. Zheng, W. Liang, M. Hada, M. Ehara, K. Toyota, R.

Fukuda, J. Hasegawa, M. Ishida, T. Nakajima, Y. Honda, O. Kitao, H. Nakai, T. Vreven, K. Throssell, J. A. Montgomery, Jr., J. E. Peralta, F. Ogliaro, M. Bearpark, J. J. Heyd, E. Brothers, K. N. Kudin, V. N. Staroverov, T. Keith, R. Kobayashi, J. Normand, K. Raghavachari, A. Rendell, J. C. Burant, S. S. Iyengar, J. Tomasi, M. Cossi, J. M. Millam, M. Klene, C. Adamo, R. Cammi, J. W. Ochterski, R. L. Martin, K. Morokuma, O. Farkas, J. B. Foresman, and D. J. Fox, Gaussian, Inc., Wallingford CT, 2016.

21. Grosjean, S., Triki, S., Meslin, J. -C., Julienne, K., Deniaud, D. (2010) Synthesis of nitrogen bicyclic scaffolds: pyrimido[1,2-a]pyrimidine-2,6-diones. Tetrahedron, 66, 9912-9924. DOI: 10.1016/j.tet.2010.10.059.
22. Yang, G., Jia, Q., Chen, L., Du, Z., Wang, J. (2015) Direct access to pyrimidines through organocatalytic inverse-electron-demand Diels–Alder reaction of ketones with 1,3,5-triazine. RSC Adv. 5, 76759-76763. DOI: 10.1039/C5RA16995J.
23. Gayon, E., Szymczyk, M., Gérard, H., Vrancken, E., Campagne, J. -M. (2012) Stereoselective and Catalytic Access to β-Enaminones: An Entry to Pyrimidines. J. Org. Chem. 77, 9205–9220. DOI: 10.1021/jo301675g.
24. Bera, M. K., Domínguez, M., Hommes, P., Reissig, H.-U. (2014) The Flögel-three-component reaction with dicarboxylic acids - an approach to bis(β-alkoxy-β-ketoenamides) for the synthesis of complex pyridine and pyrimidine derivatives. Beilstein J. Org. Chem. 10, 394–404. DOI: 10.3762/bjoc.10.37.
25. Malik, I., Ahmed, Z., Reimann, S., Ali, I., Villinger, A., Langer, P. (2011). Synthesis and photophysical properties of alkynylated pyrimidines by site-selective sonogashira reactions of 2,4,5,6-tetrachloropyrimidine; first synthesis of tetraalkynyl-pyrimidines. Eur. J. Org. Chem. 2088–2093. DOI: 10.1002/ejoc.201001622.

26. Naseer, M. M., Hameed, D. (2012) Double Suzuki cross-coupling reaction of pyrimidine boronic acid: synthesis of new versatile dielectrophile. Appl. Organometal. Chem. 26, 330–334. DOI: 10.1002/aoc.2865.
27. Achelle, S., Ramondenc, Y., Dupas, G., Plé, N. (2008) Bis- and tris(arylethynyl)pyrimidine oligomers: synthesis and light-emitting properties. Tetrahedron 64, 2783–2791. DOI: 10.1016/j.tet.2008.01.037.
28. Rodríguez-Aguilar, J., B. Ordóñez, M. Vidal, M.C. Rezende, M. Domínguez (2017) Microwave-Promoted Synthesis of 4-Arylpyrimidines by Pd-Catalysed Suzuki–Miyaura Coupling of 4-Pyrimidyl Tosylates in Water. SynOpen 1, 24–28. DOI: 10.1055/s-0036-1588810.
29. Nakao, K., H. Sasabe, R. Komatsu, Y. Hayasaka, T. Ohsawa and J. Kido (2017) Significant Enhancement of Blue OLED Performances through Molecular Engineering of Pyrimidine-Based Emitter. Adv. Optical Mater. 5, 1600843. DOI: 10.1002/adom.201600843.
30. Itami, K., D. Yamazaki and J-I Yoshida (2004) Pyrimidine-Core Extended π-Systems: General Synthesis and Interesting Fluorescent Properties. J. Am. Chem. Soc. 126, 15396-15397.
31. Catalán J. (2009) Toward a Generalized Treatment of the Solvent Effect Based on Four Empirical Scales: Dipolarity (SdP, a New Scale), Polarizability (SP), Acidity (SA) and Basicity (SB) of the Medium. J. Phys. Chem. B 113, 5951-5960. DOI: 10.1021/jp8095727.
32. Jacquemin, D., A. Planchat, C. Adamo, B. Mennucci (2012) TD-DFT Assessment of Functionals for Optical 0–0 Transitions in Solvated Dyes J. Chem. Theory Comput. 8, 2359–2372. DOI: 10.1021/ct300326f.

33. Aliaga, C. A. Lopez de Arbina, C. Pastenes and M. C. Rezende (2018) Antioxidant-spotting in micelles and emulsions. Food Chem. 245, 240-245. DOI: 10.1016/j.foodchem.2017.10.094

Table 1. Emission energy values[†] in kcal·mol^{-1} for diazines **1a–g** in various protic and non protic solvents.

Solvent	**1a**	**1b**	**1c**	**1d**	**1e**	**1f**	**1g**
Hexane	67.27	66.49	67.59	65.73	66.18	66.03	75.44
Benzene	62.98	62.98	63.96	64.39	64.69	64.69	73.31
Dichloromethane	55.73	55.41	56.39	55.84	56.73	56.95	68.24
Chloroform	58.59	58.47	59.32	58.83	59.32	59.07	70.77
Acetonitrile	52.17	52.17	52.75	53.34	53.84	53.54	65.13
DMF	52.08	52.36	52.95	53.64	54.46	53.74	65.28
DMSO	50.87	50.69	51.89	53.24	53.54	53.44	64.25
1-octanol	54.67	54.56	54.88	56.73	57.88	57.99	67.91
1-butanol	53.44	53.34	53.44	54.46	54.98	54.56	65.73
2-propanol	53.34	53.44	53.24	53.84	54.46	54.15	65.43
Ethanol	53.24	53.04	53.04	53.54	53.95	53.84	64.54
Methanol	53.64	53.14	52.46	53.24	53.04	53.04	62.02

[†] Excitation λ_{max} values were 365 nm for compounds **1a**–**f** and 330 nm for compound **1g**.

Table 2. Values for the fitting parameters *a*, *b*, *c* and *d* in the multiparametric Equations 1 and 2 (see bellow), calculated by the regression analysis of the experimental energy values of Table 1.

Diazine	E_{em}^{0}	*a*	*b*	*c*	*d*	r^{2} †
1a††	68.36±3.6	0.43±2.5	-6.17±1.3	-2.15±5.0	-12.15±1.1	0.96
1a†††	66.85±0.7	-	-5.85±0.9	-	-12.26±1.0	0.97
1b††	67.48±3.7	-0.31±2.5	-5.65±1.3	-1.61±5.2	-11.83±1.1	0.95
1b†††	66.36±0.7	-	-5.66±1.0	-	-11.91±1.0	0.96
1c††	67.10±3.4	-2.32±2.3	-5.74±1.2	0.51±4.7	-12.14±1.0	0.97
1c†††	67.47±0.7	-	-6.68±1.0	-	-12.12±1.0	0.97
1d††	62.32±3.2	-1.17±2.2	-3.68±1.2	5.72±4.5	-11.67±1.0	0.96
1d†††	66.35±0.8	-	-4.52±1.0	-	-11.38±1.1	0.95
1e††	63.08±2.6	-2.63±1.7	-2.79±0.9	5.39±3.6	-11.90±0.8	0.97
1e†††	66.88±0.8	-	-4.19±1.1	-	-11.63±1.1	0.95
1f††	62.03±2.5	-1.62±1.7	-3.16±0.9	6.91±3.4	-12.19±0.7	0.98
1f†††	66.89±0.7	-	-4.26±1.0	-	-11.84±1.1	0.95
1g††	73.96±2.1	-5.70±1.4	-2.19±0.7	3.07±2.9	-9.81±0.6	0.98
1g†††	76.16±0.9	-	-4.62±1.3	-	-9.66±1.3	0.90

† Squared correlation coefficient between calculated and experimental values. †† Regression equation 1; ††† regression equation 2;

Table 3. Experimental and calculated emission energies, in kcal.mol^{-1}, for diazine **1a** in three solvents of different polarity.

Entry	Solvent	E_{em}^{exp}	E_{em}^{calc} †
1	Benzene	67.27	69.17
2	Dichloromethane	55.63	59.55
3	Dimethylsulfoxide	50.87	56.26

†Calculated at the CAM-B3LYP/6-31+G(d) level of theory employing the SCRF=PCM option for solvent effects.

Table 4. Emission λ_{max} and quantum-yield values for compounds **1a** and **1d** in methanol, benzene and an aqueous micellar solution of reduced Triton X-100.

Compound	Emission λ_{max} † in micelle	Quantum yields in different media, Φ		
		micelle	methanol	benzene
1a	452	0.559 ±0.005	0.0032 ±0.0013	0.758 ±0.003
1d	452	0.878 ±0.001	0.0298 ±0.0009	1.000 ±0.001

† In nm, excitation at 365 nm

Table 5. Stern-Volmer constants for the quenching of dyes **1a** and **1d** by radicals **12a-c** in an aqueous solution of Triton X-100.

Dye	Radical quencher	
	12a	**12b**
1a	859 ± 26	1125 ± 23
1d	737 ± 8	1150 ± 14

FIGURE AND SCHEME CAPTIONS

Scheme1. Structures of all studied diazines **1a**-**g**

Scheme 2. General synthetic route for the preparation of diazines **1a**–**g**.

Figure 1. Absorption (solid black, λ_{max} = 380 nm), emission (dashed black λ_{max} = 563), excitation (solid red, λ_{max} = 331 and solid blue 371 nm) and emission spectra (dashed red, λ_{max} = 432 and dashed blue 563 nm) of 1a in DMSO. In the inset, absorption spectra of **1a** in hexane (solid purple, λ_{max} = 358 nm), DMSO (solid black, λ_{max} = 371 nm) and methanol (solid green, λ_{max} = 363 nm)

Figure 2. Emission spectra of diazine **1a** (λ_{exc} = 365 nm) in *n*-hexane (red), benzene (blue), trichloromethane (dark green), dichloromethane (black), 1-butanol (pink), dimethylsulfoxide (DMSO) (light blue) and aqueous micelle solution (light green).

Scheme 3. Canonical structures of the resonance hybrids of dyes **1a**–**g** in the ground and in the first excited state.

Figure 3. Linear correlation (r^2 = 0.97) for compound **1a**, between the emission energy values (E_{em}^{calc}), calculated with the aid of equation 2, and the experimental energy values (E_{em}^{exp}) in twelve solvents.

Figure 4. Electron densities of the ground (left) and excited (S_1) (right) states of dye **1a** calculated in dichloromethane.

Scheme 4. Structures of the 4-alkanoyloxyTEMPO radicals employed in the quenching experiments.

Figure 5. Stern-Volmer plots for the quenching of (a) dye **1a** by radical **12b**, and (b) dye **1d** by radical **12a**.

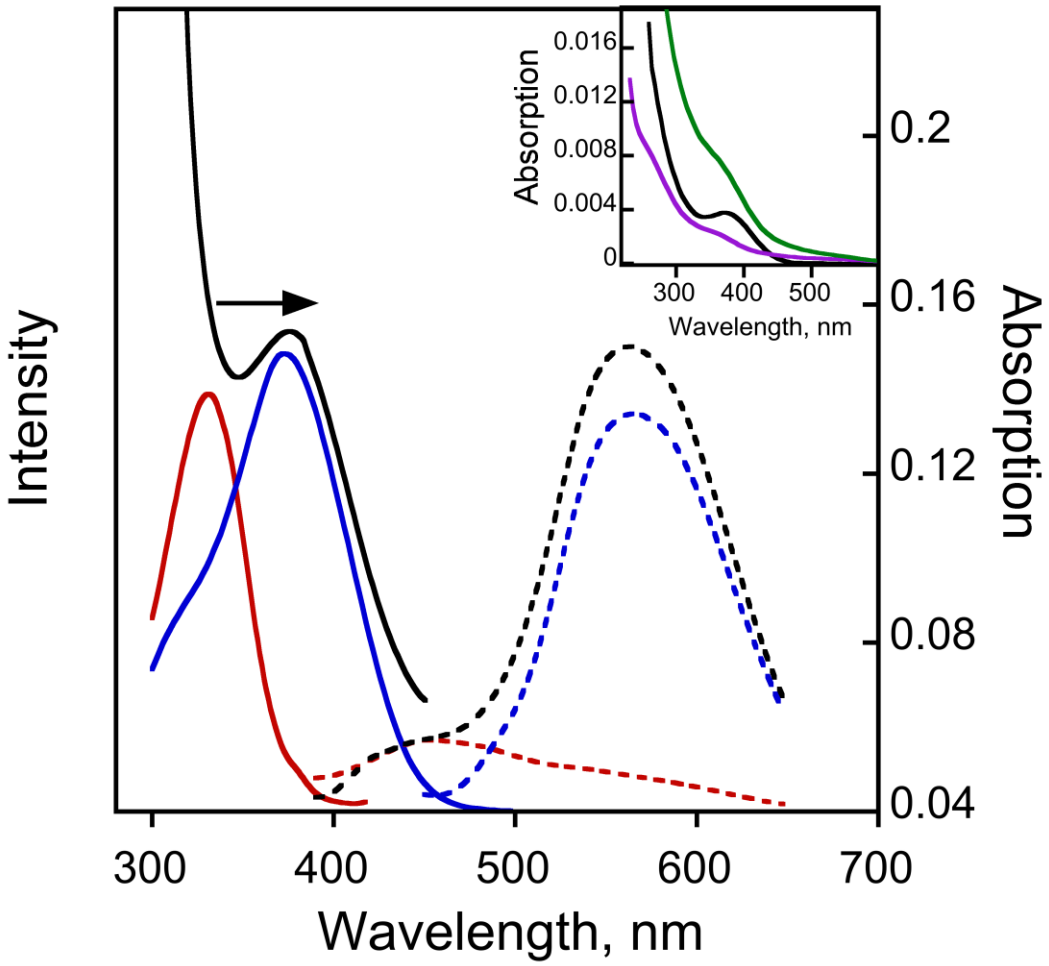

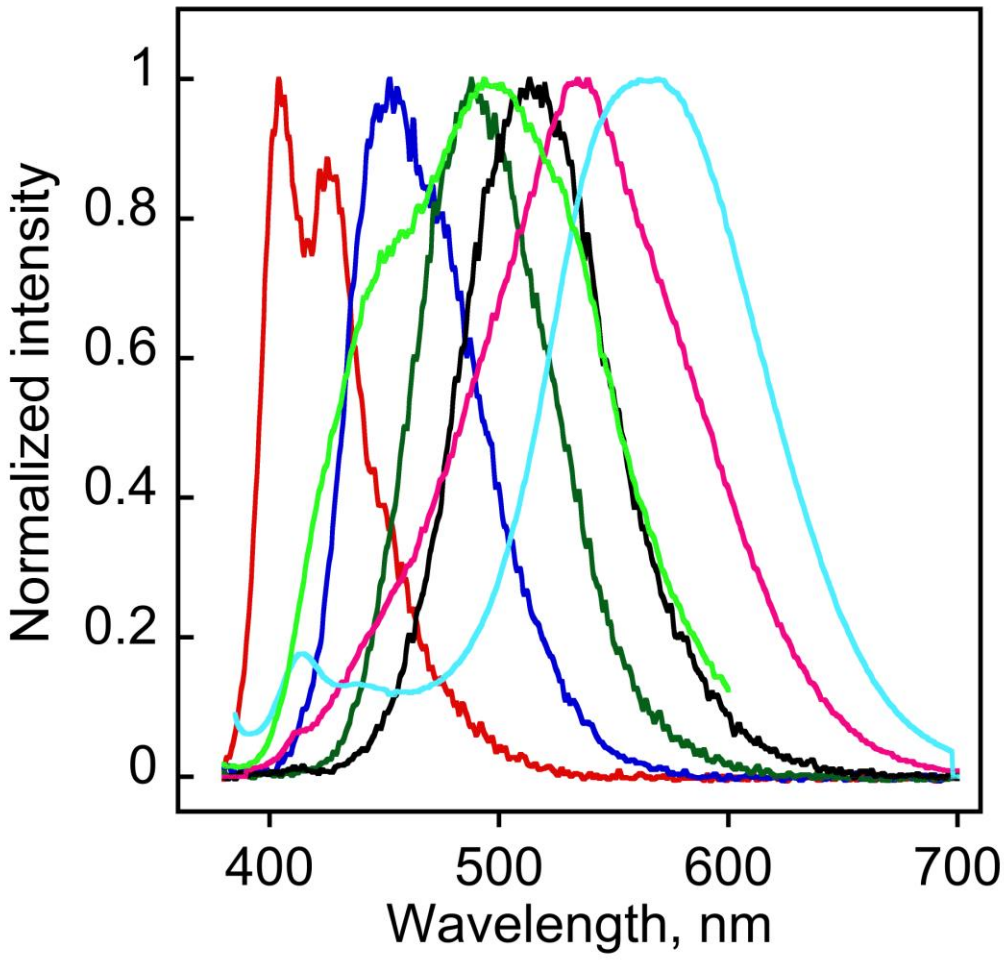

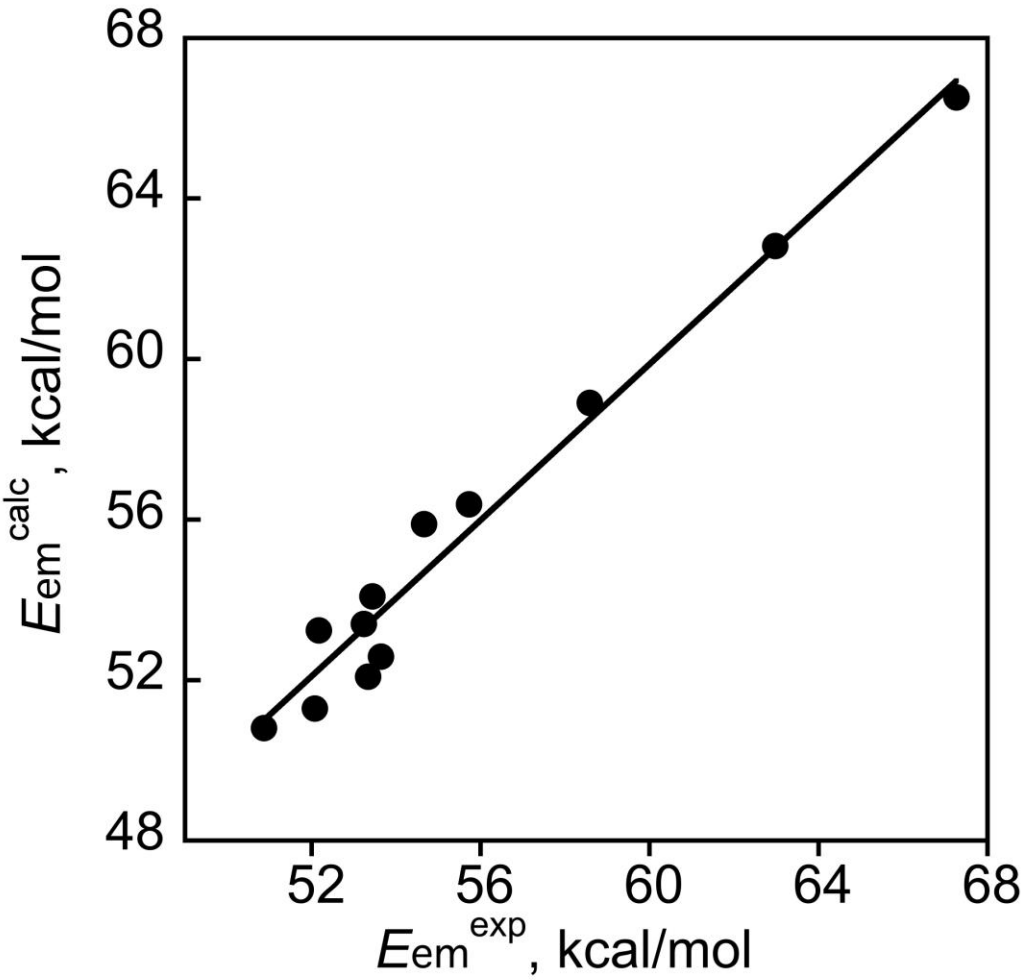

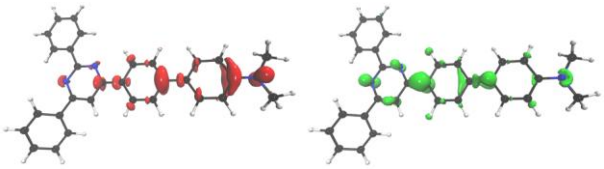

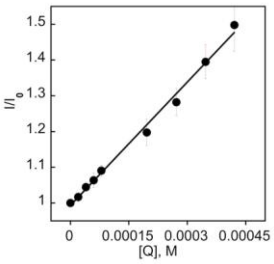

a

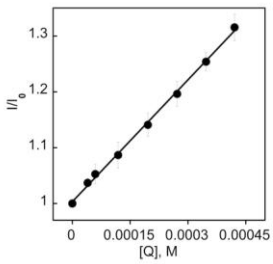

b

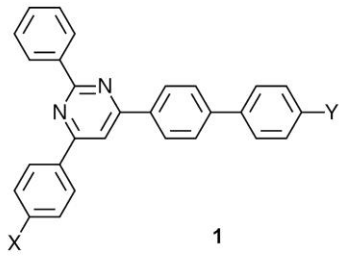

1

	a	b	c	d	e	f	g
X	H	F	OMe	H	F	OMe	H
Y	NMe_2	NMe_2	NMe_2	NPh_2	NPh_2	NPh_2	OMe

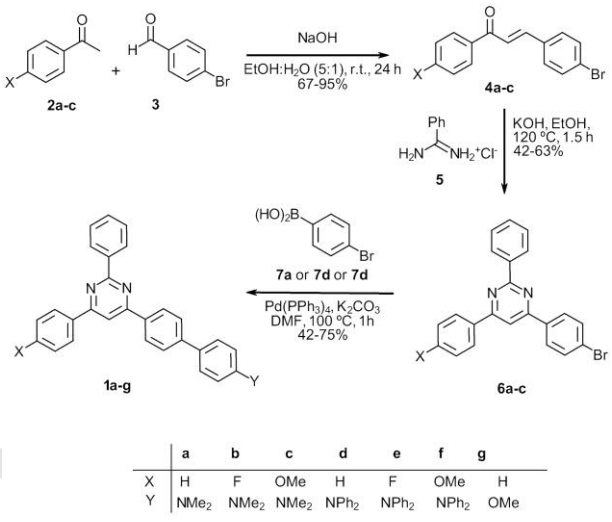

	a	b	c	d	e	f	g
X	H	F	OMe	H	F	OMe	H
Y	NMe_2	NMe_2	NMe_2	NPh_2	NPh_2	NPh_2	OMe

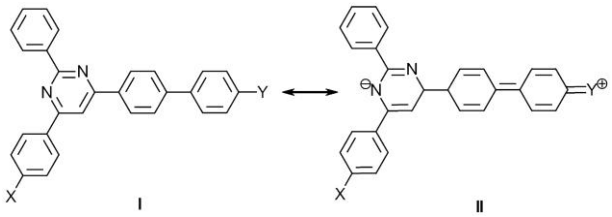

I II

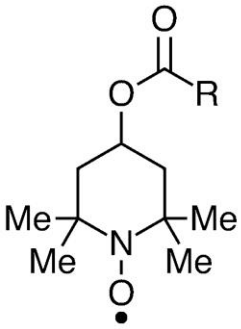

R= CH_3 (**12a**)
R= C_5H_9 (**12b**)